JOURNAL OF THERMOPHYSICS AND HEAT TRANSFER
Vol. 11, No. 1, January–March 1997

Oscillatory Thermocapillary Flow in Cylindrical Columns of High Prandtl Number Fluids

J. Masud,* Y. Kamotani,† and S. Ostrach‡
Case Western Reserve University, Cleveland, Ohio 44106

Oscillatory thermocapillary flow of high Prandtl number fluids in the half-zone configuration is investigated experimentally. Small zones (diameter ≤3 mm) are used to minimize the effects of buoyancy and gravity on the oscillation phenomenon. The effects of buoyancy and zone shape on the phenomenon are carefully assessed. The conditions for the onset of oscillations are studied under various conditions and for various zone shapes to find the dimensionless parameter(s) to specify the onset. The present data are compared with available data taken in microgravity. It is shown that for a given zone shape and fluid, the onset conditions in the absence of buoyancy cannot be specified by the Marangoni number alone.

Nomenclature

Ar = aspect ratio, L/D
Bd = dynamic Bond number, $Gr/R\sigma$
Bi = Biot number, hL/k
Bo = static Bond number, $\rho gL^2/\sigma$
Ca = capillary number, $\sigma_T \Delta T/\sigma$
D = liquid column base diameter
Do = liquid column neck diameter
Dr = column diameter ratio, Do/D
Gr = Grashof number, $g\beta\Delta TL^3/\nu^2$
h = heat transfer coefficient at free surface
k = fluid thermal conductivity
L = liquid column length
Ma = Marangoni number, $PrR\sigma$
Ma_{cr} = critical Marangoni number
Pr = Prandtl number, ν/α
R = column base radius, $D/2$
R_s = radial location of liquid free surface
$R\sigma$ = surface tension Reynolds number, $\sigma_T \Delta TL/\mu\nu$
(r, z) = coordinate system, Fig. 1
T = temperature
T_c = cold wall temperature
T_h = hot wall temperature
U_r = reference velocity
u = velocity component in z direction
α = thermal diffusivity
β = coefficient of thermal expansion
ΔR_s = dynamic free surface deformation
ΔT = $T_h - T_c$
ΔT_{cr} = critical temperature difference
μ = dynamic viscosity
ν = kinematic viscosity
ρ = density
σ = surface tension
σ_T = temperature coefficient of surface tension

Introduction

THERMOCAPILLARY flow is known to become oscillatory under certain conditions. Much attention has been given lately to oscillatory thermocapillary flow, mainly because its cause is not yet fully understood. Ever since the transition was found by Schwabe et al.[1] and Chun and Wuest[2] in the so-called half-zone simulation of the floating zone crystal growth process, in which a liquid column is suspended between two differentially heated rods, many investigators have studied the phenomenon under various conditions, both experimentally and theoretically. Among numerous studies on the subject in literature, those pertinent to the present work include experimental work by Refs. 3–9. Much of the past work was done in the half-zone configuration, and high $Pr > 1$ fluids were used in most experiments.

Despite all of the past work, questions still remain concerning the physical mechanism of oscillations and the parameter(s) defining their onset. Experimentally, for a given test fluid and zone dimensions, the flow becomes oscillatory beyond a certain critical temperature difference across the column length. It can be shown from dimensional analysis that the only parameter containing the temperature difference is Ma, if the liquid free surface is assumed to be undeformable. Therefore, many investigators assumed that the transition is characterized by a critical Ma_{cr}. Past ground-based experiments with small zones (less than 1 cm in diameter) suggest that Ma_{cr} is around 10^4 for high Pr fluids. However, experimental data taken in microgravity with larger zones have become available recently,[10,11] and they show that Ma_{cr} increases with the zone dimensions, which contradicts the assumption that Ma_{cr} alone can specify the transition. The fact that Ma alone cannot characterize the onset of oscillations was found also in our earlier ground-based experiments on the half-zone,[4] as well as in our space experiment on thermocapillary flow in cylindrical containers.[12,13] Therefore, at least one more dimensionless parameter in addition to Ma is needed to characterize the oscillation phenomenon in high Pr fluids.

The fact that Ma alone cannot specify the onset of oscillations in high Pr fluids has not been widely accepted, and Ma_{cr} is still being used in many experiments and analyses. There are various reasons for that.

1) Ground-based experiments are conducted in limited parametric ranges (Ma is of the order of 10^4).

2) Some experimental data are confusing because of buoyancy, zone shape, and rapid heating rate, etc.

3) Theoretical linear stability analyses with undeformable free surface (e.g., Neitzel et al.[7] and Kuhlmann and Rath[8]) predict Ma_{cr} that seem to agree with some of the available ground-based experimental data.

4) Most of the data taken in microgravity are not widely available.

Received Jan. 22, 1996; revision received July 1, 1996; accepted for publication July 16, 1996.

*Graduate Research Assistant, Department of Mechanical and Aerospace Engineering.
†Professor, Department of Mechanical and Aerospace Engineering. Associate Fellow AIAA.
‡Professor, Department of Mechanical and Aerospace Engineering. Fellow AIAA.

The present work is initiated to more carefully examine aspects such as buoyancy effects and interface shapes. Considerable scatter among various data is in part responsible for confusion about the causes of the oscillations. The onset conditions of oscillations are herein measured in half-zones, with careful attention to those effects, and together with available data taken in microgravity, it is shown clearly that Ma alone cannot specify the onset of oscillations for high Pr fluids.

Important Dimensionless Parameters

A vertical liquid bridge is formed between two cylindrical metal rods as shown in Fig. 1. The temperatures of top and bottom rods are maintained at constant but different values, T_h and T_c, respectively. If the free surface is flat and undeformable, the important dimensionless parameters for steady flow in the presence of buoyancy are[14] $R\sigma$, Gr, Pr, and Ar. The Marangoni number is defined as $Ma = R\sigma Pr$. The ratio of buoyancy to thermocapillary forces is represented by $Gr/R\sigma$, which is called B_d.

In the present study, the total fluid volume is varied to obtain various column shapes. The static free surface shape (in the absence of fluid motion) is determined by the total fluid volume, the column dimensions L and D, and $Bo = \rho g L^2/\sigma$. The free surface is always pinned at the edge of each rod in the present experiment, and its shape is nearly flat or close to a circular arc, as depicted in Fig. 1. As will be shown later, for the oscillation phenomenon, the ratio of the liquid column minimum diameter (maximum diameter in the case of convex free surfaces) to the base diameter D_0/D, called Dr is important. Therefore, Dr is used herein to express the column shape. When the free surface is nearly flat, it has slightly concave as well as slightly convex regions in the presence of gravity, in which case D_0 is taken as the average of the minimum diameter in the concave region and the maximum diameter in the convex region.

When there is fluid motion in the liquid column, the surface shape changes, and the deformation is represented by the capillary number ($Ca = \mu U_r/\sigma$, where U_r is the characteristic velocity of the flow). Ca expresses the ratio of viscous normal stress to surface tension at the surface and is a good measure of surface deformations when the flow is viscous dominated. As will be shown later, the flow is viscous dominated in the parametric ranges of the present experiment, even though $R\sigma$ is much larger than unity. Therefore, we use Ca herein, and for the viscous-dominated case, U_r scales with $\sigma_T \Delta T/\mu$ (Ref. 14), so that Ca can be expressed as $Ca = \sigma_T \Delta T/\sigma$.

One more parameter is needed to represent the heat loss from free surface to ambient air. The heat loss is mainly through natural convection, forced convection (caused by free surface motion), and radiation. For simplicity, the total heat loss is represented by h herein, and h is nondimensionalized as hL/k (called Bi).

Experiments

The experimental setup used in the present work is similar to the one used in our past experiments.[4] The top and bottom rods are supported by a system that can position and align them accurately. The rods are made of copper. Two rod diameters (2 and 3 mm) are used. The test fluids (silicone oils) are very wetting on copper surfaces. To prevent the fluid from wetting the outside surface of the rod, the rod edge is made sharp, as illustrated in Fig. 2. The top rod is heated by a nichrome wire wound around the rod, and the bottom rod is cooled by circulating water from a constant temperature bath (Fig. 2). The temperature of each rod is monitored by a thermocouple inserted into it.

The test fluids are 2- and 5-cSt silicone oils manufactured by Dow Corning. The thermophysical properties of the fluids are supplied by the company. The fluid is placed between the rods by a hypodermic syringe. The fluid is mixed with a small amount of alumina particles (1–20 μm size) for flow visualization. A video camera with a macro lens (a magnification of more than 50 times) is used to observe the tracer particles as well as to determine the exact shape of the liquid column.

The parametric ranges covered by the experiments are $Ma < 2.5 \times 10^4$, $20 < Pr < 60$, $0.3 \leq Ar \leq 1.0$, $0.4 \leq Dr \leq 1.2$, $Bd \leq 1.0$, and $Bo \leq 2.0$, where the properties are evaluated at the mean temperature $(T_h + T_c)/2$. Since the values of Bd and Bo are not much less than unity, gravity and buoyancy cannot be neglected completely, and so we will assess the effects of those parameters on the steady flow by numerical analysis later. The effect of surface heat loss (Bi) will also be discussed later.

The experimental procedure is the same as in our earlier study.[4] Before each test the rods are carefully cleaned and dried. A barrier coating is applied over the outside surface of each rod. After a desired amount of fluid is placed between the rods, the heater power is increased stepwise. Typically, two runs are made to find the ΔT_{cr} for the onset of oscillations. First, a coarse run with temperature steps of about 1–2°C is made to obtain a general estimate of ΔT_{cr}. A second run starts also with 1–2°C increments, but, near ΔT_{cr}, the increment is reduced to 0.2–0.3°C. At each power setting enough time is allowed for the system to reach a steady-state judging from the rod temperatures and the flowfield. It is also important that the contact line condition is checked carefully throughout a run, because the wetting of the rod edge by the fluid influences the onset of oscillations. At the onset of oscillations the flow structure undergoes a distinct change, as reported previously by several investigators,[3] so that the onset can be determined by flow visualization.

The experimental error in the temperature measurement is estimated to be ±0.1°C. The value of ΔT_{cr} is found to be reproducible within ±0.5°C. The error in the positioning and alignment of the rods is estimated to be less than 5% of the rod diameter.

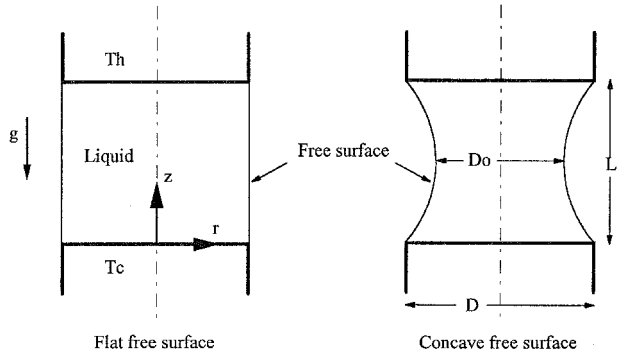

Fig. 1 Half-zone configuration with flat and curved free surfaces.

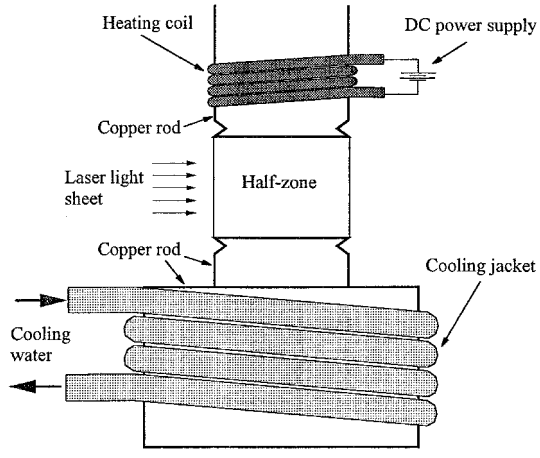

Fig. 2 Schematic of experimental arrangement.

Analysis

Numerical Analysis

Numerical analysis is performed to supplement the experiment in describing the basic flowfield. The analysis is done only for steady flow with a flat and fixed free surface. The analysis is based on the SIMPLER algorithm by Patankar[15] as in our past numerical analysis on steady thermocapillary flows.[12,13] The flow is assumed to be laminar, incompressible, and axisymmetric. The fluid properties are considered to be constant in the analysis, except for viscosity and surface tension, which vary with temperature. The velocity and stream function (in cylindrical coordinates) are nondimensionalized by $\sigma_T \Delta T/\mu$ and $\sigma_T \Delta T R^2/\mu$, respectively. The temperature is made dimensionless as $(T - T_c)/\Delta T$. As in our past work, a nonuniform grid system is adopted with meshes graded toward the hot and cold walls and toward the free surface. In the present configuration, an accurate resolution of the surface velocity distribution near the hot wall is an important requirement for the numerical grid.[12,13] For the conditions of $Ma = 10^4$, $Gr = 210$, $Pr = 27$, and $Ar = 0.7$ (near the maximum Ma and Gr for the steady flow in the present experiment), the values of maximum surface velocity near the hot wall computed with three different grids 31 × 37 (radial × axial), 40 × 46, and 60 × 80, with the smallest axial mesh next to the heater of 0.006, 0.002, and 0.0005, are 0.0379, 0.0378, and 0.0378, respectively. The values of maximum stream function are 1.52×10^{-3}, 1.49×10^{-3}, and 1.48×10^{-3}, respectively. Therefore, the 40 × 46 grid is used in the present analysis.

Free Surface Shape

The free surface shape in the present experiment is discussed first. In the absence of fluid motion, the free surface shape (static free surface) is described by the following meniscus equation:

$$P_0 = \sigma \left(\frac{1}{R_s} - \frac{d^2 R_s}{dz^2} \right) + \rho g z$$

where it is assumed that $(dR_s/dz)^2 << 1$, and P_0 is a constant to be determined to obtain a desired total volume in the liquid column. The boundary conditions are $R_s(z = 0) = R_s(z = L) = R$. The largest Bo in the present experiment is 2.0 with $Ar = 0.7$, and the smallest is 0.3 with $Ar = 0.4$. The static shapes computed for those two cases are shown in Fig. 3a, where the total liquid volume in each case is equal to that of flat free surface, so that both surfaces become flat in the absence of gravity. With gravity the hydrostatic pressure in the liquid column distorts the shape, but, as Fig. 3a shows, the deviation of the static free surface from flat shape caused by gravity is at most ±2% in the present experiment.

The free surface shape changes once thermocapillary flow is started. Three factors are responsible for the change. First, the nonuniform pressure field of the flow deforms the shape with the amount of deformation being represented by Ca. Secondly, the surface tension changes along the free surface, increasing toward the cold end. The relative surface tension variation is given by $\sigma_T \Delta T/\sigma$, which is the same as the expression for Ca. In the present analysis the dynamic free surface deformation is determined by domain perturbation, namely, the meniscus equation is solved using the pressure and viscous normal stress at the flat free surface, which are obtained in the numerical analysis with the rigid and flat free surface.[16] The computed free surface deformation from the static shape caused by the previous two effects for the conditions of $Ma = 10^4$, $Gr = 170$, $Pr = 55$, $Ar = 0.7$, and $Ca = 0.1$, is presented in Fig. 3b. The figure shows that the maximum deviation from the static shape is less than 0.1%. The third factor is that the fluid expands as it is heated. Measurement of the free surface shape near the onset of oscillations in experiments will include thermal expansion because the fluid is already heated. In summary, the distortion of the free surface shape in the present nearly flat surface tests is mainly caused by gravity and the distortion is less than ±2% from the shape in 0-g.

Basic Flowfield

Some important features of steady thermocapillary flow near the onset of oscillations can be discussed based on the numerical analysis. The computed velocity and temperature fields for typical steady thermocapillary flow with a flat static free surface are shown in Fig. 4. The flow structure (Fig. 4a) is unicellular (toroidal cell) with the cell center located near the corner of the hot wall and the free surface. In the following discussion, the flow along the free surface toward the cold wall and the interior flow toward the hot wall are called the surface flow and the return flow, respectively. Since Ma is much larger than unity, convection is important, which causes thin thermal boundary layers along the hot and cold walls, the one along

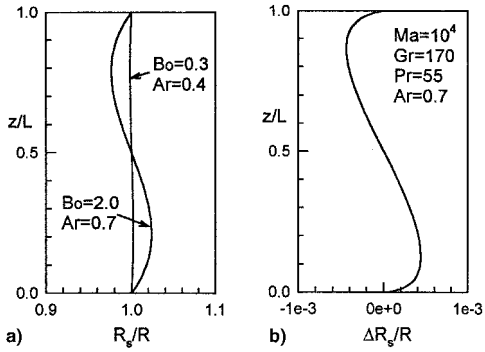

Fig. 3 a) Static and b) dynamic free surface deformation.

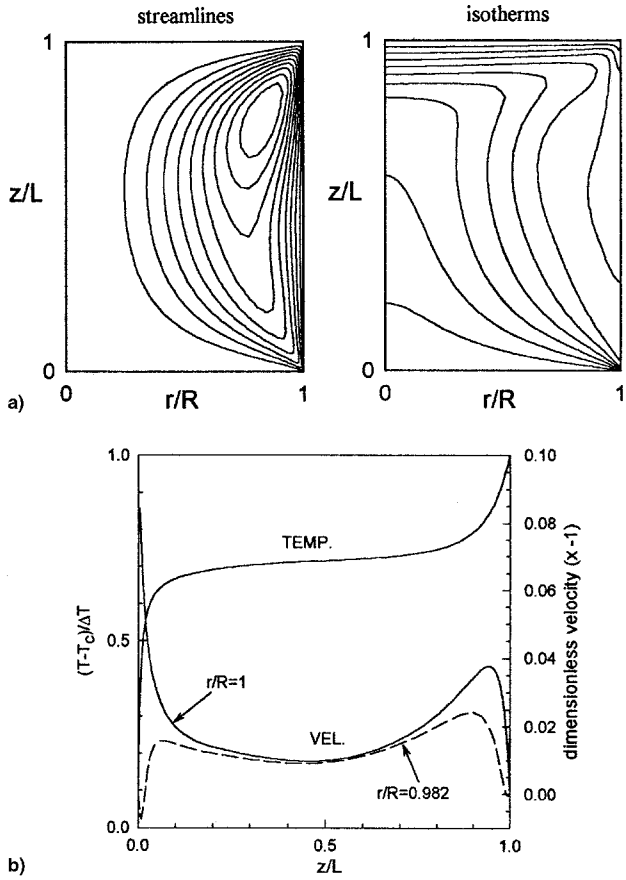

Fig. 4 Basic flow and temperature field ($Ma = 10^4$, $Gr = 210$, $Pr = 27$, and $Ar = 0.7$): a) overall flow structure and b) axial velocity and temperature distributions.

the hot wall being seen clearly in the isotherm pattern (Fig. 4a).

Because of the boundary layers, the temperature distribution along the free surface has the profile shown in Fig. 4b: sharp temperature drops in relatively small regions near the hot and cold walls and a relatively uniform distribution in between, called an S-shaped profile herein. Those regions near the walls are called the hot- and cold-corner regions. Since the surface temperature gradient is directly related to thermocapillary force, the driving force is large in those corner regions and the surface velocity distribution has a peak in each region (Fig. 4b). The peak surface velocity is larger in the cold-corner region than that in the hot-corner region, as convection along the free surface toward the cold wall causes a much larger temperature gradient in the former region. However, the driving force near the cold wall is much less effective in generating the overall flow than that near the hot wall, because the flow is driven toward the wall in the cold corner, which tends to reduce the size of the driving force region by convection when *Ma* is large. Therefore, the peak velocity in the cold-corner region disappears away from the free surface, as the axial velocity at $r/R = 0.982$ shows in Fig. 4b. The fact that the hot-corner region is mainly driving the overall flow explains why the toroidal cell center is located near the hot wall in Fig. 4a. The numerical analysis shows that the hot-corner region shrinks with increasing *Ma*, as the thermal boundary layer along the hot wall becomes thinner.

Another very important feature of the flow is that it is viscous dominated in the parametric ranges where the flow is known to become oscillatory in the 1-*g* tests. That can be shown numerically by comparing the flowfields computed with and without the inertia terms in the momentum equations. For the conditions of Fig. 4, the value of Reynolds number is $R\sigma = 370$, which is close to the largest Reynolds number at the onset of oscillations in the present near-flat surface tests, and the computed dimensionless maximum stream function and maximum surface velocity in the hot corner are 1.49×10^{-3} and 0.0378, respectively, with the inertia terms, and 1.45×10^{-3} and 0.0376, respectively, without the inertia terms, so that they are very close. The reason for the dominance of viscous forces over inertia forces even at $R\sigma = 370$ is that the driving force (the surface temperature distribution) is altered by the flow in such a way as to narrow the important driving force region with increasing *Ma*, as discussed earlier, which is a characteristic of thermocapillary flows of high *Pr* fluid. Consequently, the dimensionless fluid velocity becomes much less than unity, as the velocity near the free surface in Fig. 4b shows. The fact that the inertia forces are negligible at the onset of oscillations, at least in the parametric ranges of the present ground-based tests, is very important because it shows that the oscillation phenomenon is not caused by a type of hydrodynamic instability in which inertia forces play an important role.

Buoyancy affects the thermocapillary flow. *Bd*, which represents the ratio of buoyancy to thermocapillary forces, is independent of ΔT and viscosity ($Bd = \rho g \beta L^2/\sigma_T$). The value of *Bd* for the conditions of Fig. 4 is 0.6 (*Bd* is less than unity in all of the present tests). In the present configuration, with the fluid heated from above, the overall flow is retarded by buoyancy. According to the numerical analysis, the streamline pattern for the conditions of Fig. 4, but with $Gr = 0$, is similar to that shown in Fig. 4a with buoyancy, but the maximum stream function is 12% larger and the maximum surface velocity in the hot corner is 1.5% larger without buoyancy. For the smallest *Bd* near the onset of oscillations in the present experiment $Bd = 0.09$, the difference in the maximum stream function is reduced to 3%. How this change in the basic flow by buoyancy affects the oscillation phenomenon will be discussed later.

We will make a simple estimate of the amount of heat loss from the free surface as follows. The heat loss is caused by radiation and convection to ambient air. The motion of the ambient air is induced by buoyancy as well as by the liquid free surface motion. It is estimated that each of those two factors produces roughly the same air velocity. For the conditions of Fig. 4, which cause the largest heat loss, the air velocity caused by either factor is estimated to be about 1 cm/s, and the value of *Bi* caused by radiation and either type of convection is estimated to be about 0.25. *Bi* represents the ratio of heat loss to conduction through the liquid column. Since convection through the column is more important than the conduction (the ratio is called *Nu*) in the present parametric ranges, the relative heat loss is estimated properly by *Bi*/*Nu*, which is about 0.04 for the previous case. Therefore, although the previous two types of air convection interact in a complex way (they oppose each other), the combined effect is not expected to have much influence on the flow in the present experiment. By forcing an airflow around the experiment, the airspeed around the liquid column was found to be at least 10 cm/s for it to affect the liquid flow near the onset of oscillations.

Experimental Results and Discussion

Once the imposed ΔT reaches a critical value (ΔT_{cr}), the flow suddenly becomes three dimensional, and both the fluid motion and the temperature oscillate temporally and spatially. Since the oscillatory flow structure has been investigated previously,[3,5] the main interest of the present study is to find the proper dimensionless parameter(s) to characterize the onset of oscillations. Therefore, the oscillatory flow is only briefly described here, which helps to interpret the present data. Although the flow is generally three dimensional, an important feature is that in a fixed radial plane (*rz* plane in Fig. 1) the surface flow becomes alternately fast and slow in one cycle of the oscillations,[4] those periods being called the active and slow periods, respectively, herein. Generally, the pattern rotates around the column axis, that is, the active and slow periods occur at different times at different radial planes. After an active period in one radial plane, the return flow in that plane is directed toward the hot region where the surface flow is just beginning to be active, which results in the characteristic interaction between two diametrically opposed cells when one cross section of the column is illuminated for flow visualization.[3] The predominant flow structure near the onset of oscillations in the present experiment has one periodic variation in the azimuthal direction (azimuthal wave number = 1). Some other modes are possible under different conditions.[5]

Shape Effect

The effect of the static free surface shape on ΔT_{cr} is investigated first. The values of ΔT_{cr} measured for various shapes and aspect ratios are shown in Fig. 5. As seen in the figure,

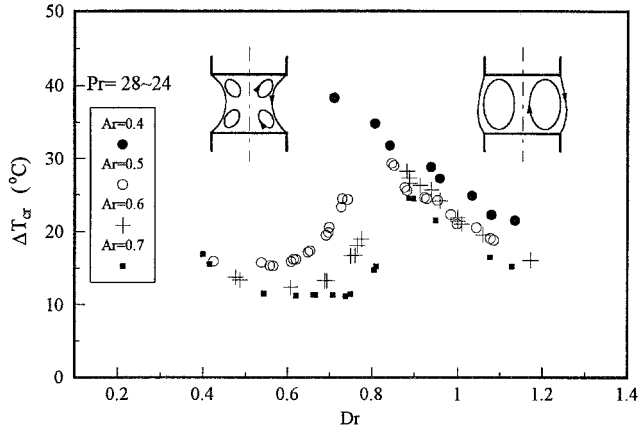

Fig. 5 Effect of free surface shape on critical temperature difference.

ΔT_{cr} is sensitive to the column neck diameter (or Dr). As Dr is decreased starting from a convex free surface ($Dr > 1$), ΔT_{cr} increases noticeably. The increase is because the average column diameter decreases with decreasing Dr and, consequently, the overall flow is observed to slow down for a given ΔT, the effect similar to increasing Ar. As seen in Fig. 5, there is a sharp drop in ΔT_{cr} near a certain Dr. According to flow observations, the sudden change is associated with the appearance of corotating secondary cells as sketched in Fig. 5. Apparently, such a flow structure makes it easier for the flow to become oscillatory. As Ar is decreased, the value of Dr for the sudden change becomes smaller, and the peak ΔT_{cr} increases. In the case of $Ar = 0.4$, there is no sudden reduction, even near $Dr = 0.6$. The smallest Dr with the fluid still pinned at the rod edges is close to $(1 - Ar)$. In all cases the oscillatory flow structure is similar: the surface flow goes through active and slow periods in one cycle of oscillations and the return flow moves across the centerline to the hot corners in different radial planes.

Hu et al.[17] and Monti et al.[18] also investigated the shape effect in the half-zone configuration, but the present work covers wider conditions. Hu et al.[17] found a similar effect of the column shape on the onset of oscillations, but they inferred from the trend of their data that there exists a range of Dr where ΔT_{cr} becomes infinite (no oscillations at any ΔT). Hu et al.[17] could not take data around the peak ΔT_{cr} region, because the liquid column broke down, probably because of high ΔT (above 100°C for 10-cSt silicone oil), so that their inference has no basis. In any case, the onset of oscillations is very sensitive to the liquid column shape, so we must consider this effect when we compare available experimental data. Monti et al.[18] characterized the zone shape by the total liquid volume instead of the zone neck diameter used in the present work. However, as shown by Hu et al.,[17] both ways of specifying the shape are equivalent.

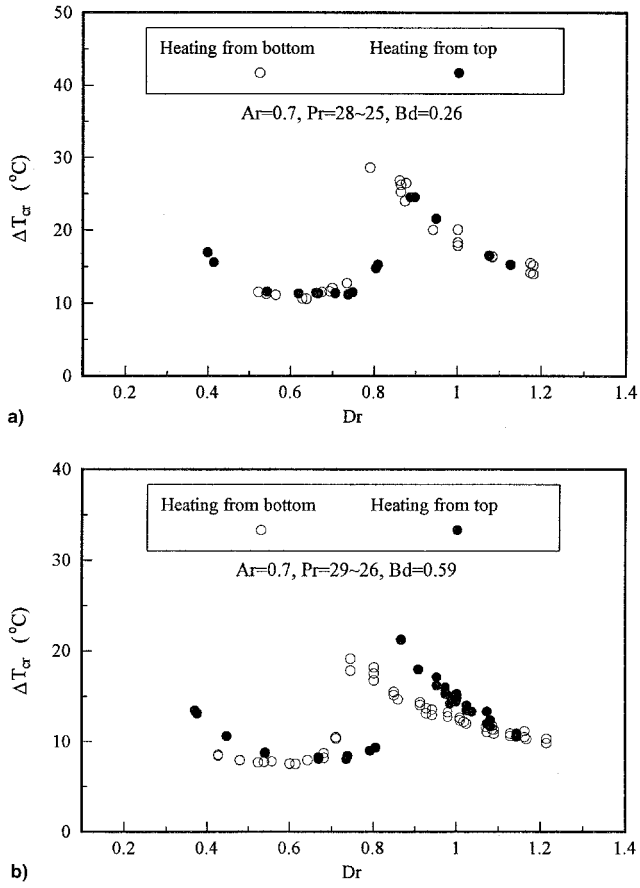

Fig. 6 Effect of heating arrangement on critical temperature difference. D = a) 2 and b) 3 mm.

Effect of Buoyancy

To study the effect of buoyancy, the tests are conducted in two configurations, one in the heated-from-above configuration (the main configuration of the present experiment) and the other in the heated-from-below configuration. The results are presented in Fig. 6 for two diameters. The results for $D = 2$ mm (Fig. 6a) with $Bd = 0.26$ show that whether the liquid is heated from below or above, ΔT_{cr} is unchanged within the experimental error and the basic flows are observed to be nearly identical, so that buoyancy is considered to have negligible influence.

The results for $D = 3$ mm are presented in Fig. 6b, in which Bd is 0.59. Figure 6b shows that when the column is heated from below, ΔT_{cr} is 10–25% smaller in the range $0.8 < Dr < 1.2$. The difference can be explained as follows. For $D = 3$ mm the free surface is not exactly flat, even when $Dr = 1$ (see Fig. 3a). According to the present numerical analysis the velocity field is influenced more by the free surface shape than by buoyancy in the parametric ranges of the present tests, which suggests that the shape effect is more important on the onset of oscillations than that of buoyancy. Consider the case with $Dr = 1$, for example. According to the shape effect, ΔT_{cr} is expected to be larger in the heated-from-above configuration than that in microgravity with flat free surface, because the free surface in 1-g is slightly concave in the hot-corner region (see Fig. 3a), whereas in the heated-from-below configuration, ΔT_{cr} is expected to be smaller since the shape is convex in the hot corner, which is consistent with the trend of the present experimental data. The fact that the effect of heating configuration decreases with increasing Dr in the range $0.8 < Dr < 1.2$ (Fig. 6b), can be explained also by the shape effect, namely as Dr increases, ΔT_{cr} becomes less sensitive to the shape in that range of Dr (Fig. 6a), so that a slight shape distortion by gravity has less influence. Since the shape effect is opposite in the two heating configurations, as explained earlier, data with negligible buoyancy are expected to fall somewhere between those two cases, and so the error in ΔT_{cr} from the present tests with $D = 3$ mm is estimated to be less than $\pm 10\%$ when the free surface is nearly flat.

Velten et al.[5] also investigated the effect of heating orientation on ΔT_{cr}. They found that the heating-from-below configuration generally increases ΔT_{cr}, contrary to the present trend. Moreover, they found that the difference in ΔT_{cr} between the two configurations becomes more noticeable as the liquid column becomes shorter, or as Bd becomes smaller, which cannot be explained by buoyancy alone. In the case of heating from below, strong upward air motion is created along the liquid surface because of the hot bottom rod. The air motion itself does not influence the oscillations but, according to our careful observations by a microscope, a very small amount of vapor from the free surface is carried upward by the air motion and condenses on the top cold rod surface. Although we did not see a visible trace of condensation on the rod after a typical test duration of about 20 min, the liquid pinning edge at the top rod was seen to become irregular as the condensation made it easier for the fluid to wet the top rod. Because of the breakdown of the sharp pinning edge, the oscillations near the onset tend to be intermittent and the value of ΔT_{cr} is not very reproducible. Therefore, in the present tests in the heated-from-below configuration, a small circular disk is placed around the bottom rod just above the heating coil (like an umbrella over the heater) to prevent the hot air from flowing along the liquid column. No such precaution was taken in the tests by Velten et al.,[5] which may explain the difference in the heating orientation effect. Velten et al.[5] also suspected that the airflow around the liquid column might have an influence on the oscillation phenomenon.

Schwabe et al.[19] conducted half-zone experiments both in 1-g and in microgravity (aboard the Space Shuttle) using the

same size liquid column (6-mm column of $NaNO_3$), and found that the onset of oscillations and the oscillation frequency were almost unchanged by the gravity level. In the experiments with $Ar = 0.8$, Bd was 0.8 and 0.8×10^{-5} in 1-g and in microgravity, respectively. The experiments show that at those values of Bd the effect of buoyancy is negligible on the oscillation phenomenon. In comparison, the maximum value of Bd in the present experiments is 1.0 and the results are consistent. The fact that buoyancy does not affect the onset of oscillations, even when Bd is not much less than unity in 1-g tests, implies that the oscillation phenomenon is driven in a relatively small region, so that the appropriate length scale to be used in evaluating buoyancy and gravity is much less than the overall L.

In summary, the effect of buoyancy on ΔT_{cr} cannot be neglected, depending on the ranges of Bd and Dr, but the effect is less than $\pm 10\%$ in the present tests with nearly flat free surfaces ($Dr = 1 \pm 2\%$).

Other Effects

Many experimental data are available concerning the onset of oscillations in the half-zones, but some of them are taken under different conditions from those studied herein. One of the test fluids used by Velten et al.[5] was KCl. The fluid is convenient because it gives data near $Pr = 1$, but since its melting point is 772°C, the radiation heat transfer from the melt to the surroundings is very high. It can be shown by numerical analysis that all of the heat transferred to the fluid at the hot wall is radiated out from the free surface in the experiment by Velten et al.[5] with KCl, a condition that is quite different from that considered herein. Paraffins (C_nH_{2n+2}) are sometimes used as test fluids, but according to Schwabe et al.[20] they are very sensitive to impurities, and so ΔT_{cr} data tend to scatter appreciably if different batches of fluid are used. In some tests aboard sounding rockets the zones were heated up too quickly, so that ΔT_{cr} was a function of the heating-up rate. Therefore, one must consider additional factors to interpret those data.

Comparison with Available Data

We now compare the present data with available experimental data. As discussed in the Introduction, the upper range of Ma is limited to be on the order of 10^4 in ground-based tests in the half-zone configuration with high Pr fluids. Therefore, we must include data taken in microgravity with larger liquid columns to cover wider ranges. Albanese et al.[10] conducted microgravity experiments during the D-2 Spacelab Mission with zone diameters of 3, 4.5, and 6 cm and Ar ranging from 0.75 to 2. They used 5-cSt silicone oil ($Pr = 65$–69) and the free surfaces were flat. Hirata et al.[11] and Haga et al.[21] conducted sounding rockets experiments with 1.5-cm half-zones of 6-cSt silicone oil ($Pr = 79$–82). We compare those results in the range $0.67 \leq Ar \leq 1$ with the present experimental data for 5-cSt silicone oil ($Pr = 54$–59) taken in the range $0.7 \leq Ar \leq 1.0$. Since the free surfaces were flat in those microgravity tests, we use the present data taken with nearly flat surfaces ($Dr = 1 \pm 2\%$). Therefore, in all of those tests, the ranges of Pr, Ar, and Dr are nearly fixed and only the zone dimension is significantly different. For that reason the values of Ma_{cr} are plotted against the zone length in Fig. 7. If Ma_{cr} alone is the sufficient parameter to specify the onset of oscillations for a given Pr, Ar, and Dr, it should not change with the zone dimensions. Figure 7 shows clearly that there is no fixed Ma_{cr}: Ma_{cr} increases appreciably with the zone dimension. Ma_{cr} varies more than one order of magnitude among those experiments, much beyond what can be explained by differences in Pr and Ar and by the effects of buoyancy and free surface shape. As discussed earlier, the value of Bi/Nu for the surface heat loss in the present experiment is estimated to be about 0.03. For the experiment by Albanese et al.[10] with $D = 6$ cm, Bi/Nu is estimated to be about 0.04, so that the heat loss effect is not much different in both tests. Therefore, it is clear that Ma_{cr} alone is not sufficient to specify the onset conditions.

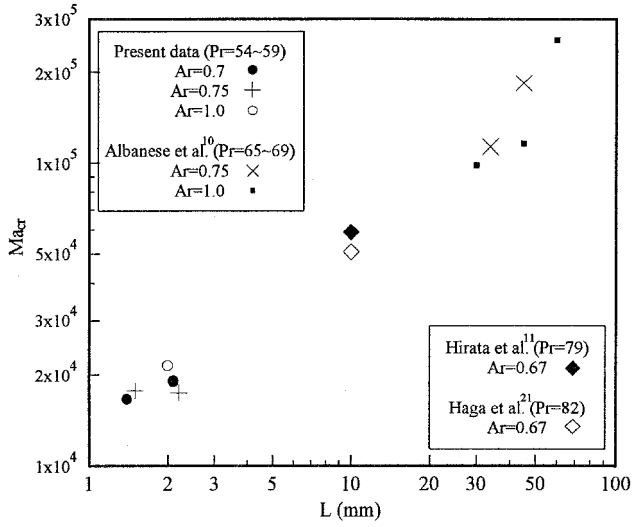

Fig. 7 Effect of zone length on critical Ma.

We also conducted thermocapillary flow experiments in microgravity with cylindrical containers,[12,13] and no oscillations were found, even though Ma was 5–7 times larger than Ma_{cr} found in our ground-based tests using smaller containers, which is consistent with the previous finding.

If the oscillation phenomenon is associated with convection, the Ma, which represents the ratio of convection to conduction heat transfer, cannot be very small at the onset of oscillations. The fact that there exists a lower bound for Ma to have oscillations can be inferred from the data by Preisser et al.[3] and Ostrach et al.[22] The data of Preisser et al.[3] with $NaNO_3$ ($Pr = 7$) show that Ma_{cr} becomes constant, equal to about 7×10^3, when the zone length is reduced while keeping the zone diameter fixed. Ostrach et al.[22] showed also that Ma_{cr} cannot go below 7×10^3 with 10-cSt silicone oil ($Pr = 100$). Therefore, one condition for the onset of oscillations is that Ma (based on L) must be larger than or equal to 7×10^3. That means that the surface temperature distribution has the aforementioned S-shaped profile.

Although the data in Fig. 7 are only in limited ranges of Pr and Ar, there are no data available in different ranges that cover a wide range of zone diameter. There are ground-based data in different ranges of Pr and Ar (including the present data), but unless all of the important dimensionless parameters are known for the onset of oscillations, there is no proper way to compare those results.

Conclusions

The conditions for the onset of oscillatory thermocapillary flow in the half-zone configuration are investigated experimentally with high Pr fluids. The effects of buoyancy and column shape on the onset conditions of oscillations are studied. Comparison of the present data with available microgravity data shows that the critical Ma generally increases with the zone dimension when buoyancy is minimized, which means that an additional dimensionless parameter is needed to characterize the onset conditions. Available data also show that there is a minimum Ma_{cr}, below which no oscillations appear, showing that convection is important for the oscillation phenomenon. Therefore, both convection and an additional feature must be taken into account together to explain the oscillation mechanism for high Pr fluids. The additional feature must be something other than the various effects investigated herein. We think free surface deformation, albeit very small, is the missing link based on our past theoretical and experimental work. A theoretical basis for that and the data correlation based on that concept will be given elsewhere.

Acknowledgments

This work was funded by NASA Grant NAG3-1568. A. Pline and T. Jacobson of the NASA Lewis Research Center were the Project Scientist and the Project Manager, respectively. The authors thank H. D. Jiang for his helpful suggestions about the experiment and K. T. Chen and M. Lin for their assistance in taking some of the data.

References

[1]Schwabe, D., and Scharmann, A., "Some Evidence for the Existence and Magnitude of a Critical Marangoni Number for the Onset of Oscillatory Flow in Crystal Growth Melts," *Journal of Crystal Growth*, Vol. 46, No. 1, 1979, pp. 125–131.

[2]Chun, C.-H., and Wuest, W., "Experiments on the Transition from Steady to the Oscillatory Marangoni Convection of a Floating Zone Under Reduced Gravity Effect," *Acta Astronautica*, Vol. 6, No. 9, 1979, pp. 1073–1082.

[3]Preisser, F., Schwabe, D., and Scharmann, A., "Steady and Oscillatory Thermocapillary Convection in Liquid Columns with Free Cylindrical Surface," *Journal of Fluid Mechanics*, Vol. 126, Jan. 1983, pp. 545–567.

[4]Kamotani, Y., Ostrach, S., and Vargas, M., "Oscillatory Thermocapillary Convection in a Simulated Floating Zone Configuration," *Journal of Crystal Growth*, Vol. 66, No. 1, 1984, pp. 83–90.

[5]Velten, R., Schwabe, D., and Scharmann, A., "The Periodic Instability of Thermocapillary Convection in Cylindrical Liquid Bridges," *Physics of Fluids A*, Vol. 3, No. 2, 1991, pp. 267–279.

[6]Shen, Y., Neitzel, G. P., Jankowski, D. F., and Mittelmann, H. D., "Energy Stability of Thermocapillary Convection in a Model of the Float-Zone Crystal-Growth Process," *Journal of Fluid Mechanics*, Vol. 217, Aug. 1990, pp. 639–660.

[7]Neitzel, G. P., Chang, K. T., Jankowski, D. F., and Mittlemann, H. D., "Linear Stability Theory of Thermocapillary Convection in a Model of the Float-Zone Crystal Growth Process," *Physics of Fluids*, Vol. 5, No. 1, 1993, pp. 108–114.

[8]Kuhlmann, H. C., and Rath, H. J., "Hydrodynamic Instabilities in Cylindrical Thermocapillary Liquid Bridges," *Journal of Fluid Mechanics*, Vol. 247, Feb. 1993, pp. 247–274.

[9]Wanschura, M., Shevtsova, V. M., Kuhlmann, H. C., and Rath, H. J., "Convective Instability Mechanisms in Thermocapillary Liquid Bridges," *Physics of Fluids*, Vol. 7, No. 5, 1995, pp. 912–925.

[10]Albanese, C., Carotenuto, L., Castagnolo, D., Ceglia, E., and Monti, R., "An Investigation on the Onset of Oscillatory Marangoni Flow," *Advances in Space Research*, Vol. 16, No. 7, 1995, pp. 87–94.

[11]Hirata, A., Nishizawa, S., Imaishi, N., Yasuhiro, S., Yoda, S., and Kawasaki, K., "Oscillatory Marangoni Convection in a Liquid Bridge Under Microgravity by Utilizing TR-1A Sounding Rocket," *Journal of the Japan Society of Microgravity Application*, Vol. 10, No. 4, 1993, pp. 241–250.

[12]Kamotani, Y., Ostrach, S., and Pline, A., "Analysis of Velocity Data Taken in Surface Tension Driven Convection," *Physics of Fluids*, Vol. 6, No. 11, 1994, pp. 3601–3609.

[13]Kamotani, Y., Ostrach, S., and Pline, A., "A Thermocapillary Convection Experiment in Microgravity," *Journal of Heat Transfer*, Vol. 117, Aug. 1995, pp. 611–618.

[14]Ostrach, S., "Motion Induced by Capillarity," *Physicochemical Hydrodynamics*, edited by D. B. Spalding, Vol. 2, V. G. Levich Festschrift Advance Publications, London, 1977, pp. 571–589.

[15]Patankar, S. V., *Numerical Heat Transfer and Fluid Flow*, McGraw-Hill, New York, 1980.

[16]Zebib, A., Homsy, G. M., and Meiburg, E., "High Marangoni Number Convection in a Square Cavity," *Physics of Fluids*, Vol. 28, No. 12, 1985, pp. 3467–3476.

[17]Hu, W. R., Shu, J. Z., Zhou, R., and Tang, Z. M., "Influence of Liquid Bridge Volume on the Onset of Oscillation in Floating Zone Convection: I. Experiments," *Journal of Crystal Growth*, Vol. 142, Nos. 3, 4, 1994, pp. 379–384.

[18]Monti, R., Castagnolo, D., Dell'Aversana, P., Desiderio, G., Moreno, S., and Evangelista, G., "An Experimental and Numerical Analysis of Thermocapillary Flow of Silicone Oils in a Micro-Floating Zone," World Space Congress, International Astronautical Federation, Paper 92-0918, Washington, DC, Aug. 1992.

[19]Schwabe, D., and Scharmann, A., "Measurements of the Critical Marangoni Number of the Laminar-Oscillatory Transition of Thermocapillary Convection in Floating Zones," *Proceedings of the 5th European Symposium on Material Sciences Under Microgravity*, Vol. 1, European Space Agency, SP-222, 1984, pp. 281–289.

[20]Schwabe, D., Scharmann, A., and Da, X., "Prandtl-Number Dependence of the Onset of Thermocapillary Flow in Floating Zones," *Advances in Space Research*, Vol. 11, No. 7, 1991, pp. 233–237.

[21]Haga, M., Maekawa, T., Kuwahara, K., Ohara, A., Kawasaki, K., Harada, T., Yoda, S., and Nakamura, T., "Effect of Electric Field on Marangoni Convection Under Microgravity," *Journal of the Japan Society of Microgravity Application*, Vol. 12, No. 1, 1995, pp. 19–26.

[22]Ostrach, S., Kamotani, Y., and Lai, C. L., "Oscillatory Thermocapillary Flows," *Physico-Chemical Hydrodynamics*, Vol. 6, Nos. 5, 6, 1985, pp. 585–599.